Numerical Methods in Civil Engineering, 8-4 (2024) 68-78

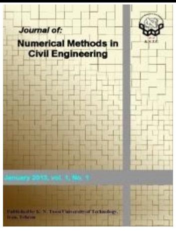

Numerical Methods in Civil Engineering

Journal Homepage: https://nmce.kntu.ac.ir/

Structural Damage Diagnosis of Reinforced Concrete Moment-Resisting Frame using Wavelet Based-Damage Sensitive Feature

Minoo Panahi Boroujeni*, Seyed Alireza Zareei, Mohammad Sadegh Birzhandi***, Mohammad Mahdi Zafarani*****

ARTICLE INFO

RESEARCH PAPER

Article history:
Received:
December 2023
Revised:
April 2024
Accepted:
July 2024

Keywords:
Damage sensitive feature
Incremental dynamic analysis
Wavelet
Reinforced concrete moment-resisting frames
Absolute acceleration response

Abstract:

This paper describes the derivation process of a wavelet-based damage-sensitive feature for structural damage diagnosis in a reinforced concrete moment-resisting frame. The wavelet-based damage-sensitive feature is based on the wavelet transform of the time-history acceleration response, obtained from incremental dynamic analysis of the floor absolute acceleration response. By applying mathematical relationships to the wavelet coefficients, the wavelet-based damage-sensitive feature is extracted as the energy of the wavelet coefficients at appropriate scales. Furthermore, the theoretical correlation between the output of wavelet analysis and dynamic structural behaviors that play a vital role in damage diagnosis methods was derived. The effectiveness of the wavelet-based damage-sensitive feature is evaluated by simulating a 4-story reinforced concrete frame subjected to various ground motion records using the continuous **bior3.3** mother wavelet family. The wavelet-based damage-sensitive feature measures changes in wavelet energy at the natural frequency of the intact structure as the damage progression occurs, and the results show that wavelet-based damage-sensitive feature values gradually decrease as damage increases.

1. Introduction

Structural Health Monitoring (SHM) methods provide detailed information on structural health prognosis in the design procedure of structures and infrastructures and performance assessment of existing ones particularly after the damage has occurred. In the field of ***SHM***, the term “damage” refers to any alterations that occur during the lifetime operation of the structure which disrupts its serviceability. In order to identify structural damage, several computational approaches which are mainly based on variation of structural dynamic behaviors including natural frequencies, transfer functions, mode responses, etc. were proposed [1, 2].

The most recent and efficient developments in damage diagnosis techniques that have gained attention were established based on the structural response signal [3-6].

One of the most effective mathematical transformations between time and frequency in the field of unsteady signal processing is wavelet transformation, which is highly capable of detecting structural damage. It is worth mentioning that the wavelet transformation consists of a set of basic functions that can analyze the input signal in both time-space and frequency-scale domains [7]. In other words, wavelet transform analysis, using the ability to decompose signals into time and frequency, provides a suitable method for processing signals that can be used as a magnifying tool to identify small changes in structures. Hence, by applying the wavelet transform analysis to the response of a damaged structure, the locations, extent, and corresponding damage state as disturbances in the wavelet coefficients diagram can be revealed. Therefore, by means of wavelet transform analysis, damage diagnosis can be easily detected by investigating the response of the damaged structures. The

** Ph.D. Candidate of Structural Engineering, Department of Civil Engineering, Isfahan (Khorasgan) Branch, Islamic Azad University, Isfahan, Iran.*

*** Corresponding author: Associate Professor of Structural Engineering, Department of Civil Engineering, Isfahan (Khorasgan) Branch, Islamic Azad University, Isfahan, Iran; E-mail: a.r.zareei@khuisf.ac.ir.*

**** Assistant Professor of Structural Engineering, Department of Civil Engineering, Isfahan (Khorasgan) Branch, Islamic Azad University, Isfahan, Iran.*

https://doi.org/10.61186/NMCE.2312.1038

studies of Hera and Hou [8], Nair and Kiremidjian [9], Aguirre et al. [10], and Balafas and Kiremidjian [11] are some of the most recent progressions to characterize the observed structural damage among many. Furthermore, this method does not require the response of similar intact structures to detect the damages that occurred to the target structure. The studies of Mallat [12], Cruz and Salgado [13], and Solís et al. [14] are some of the most prestigious and highly regarded studies that have employed wavelet transform analysis to deduce the level of structural damage at a given seismic intensity.

This study focuses on investigating the wavelet transform analysis method with the structural acceleration response for classifying or predicting structural damage of reinforced concrete moment-resisting frame (***RC-MRF***) using the wavelet-based damage-sensitive feature (***WB-DSF***). To extract the ***WB-DSF***, the absolute floor acceleration responses of the under-consideration structure subjected to ground motion stimulation were recorded. Nonlinear incremental dynamic analysis (***IDA***), a powerful tool for nonlinear analysis of structures under incremental ground motion intensity, was used to determine the structural responses, which involved applying a range of scaled ground motions to the structure to assess its seismic performance under different loading intensities [15, 16]. Thereafter, the maximum story drift ratio (***SDR***) of each story was found to identify the damaged states of the structure [17, 18]. After that by extracting and refining the acceleration responses of the models, the wavelet transformation is applied to calculate the energies of wavelet coefficients [4, 8, 19-24]. Wavelet transform, a signal processing tool, decomposes signals into frequency components for time-frequency analysis, beneficial in seismic analysis. Combining IDA with wavelet transform allows simultaneous analysis of structural response in time and frequency domains, identifying critical vibration modes. This integrated approach provides a holistic understanding of seismic performance, aiding in energy distribution assessment and overall design improvement. Leveraging both methods enhances accuracy in seismic assessments and captures a wider range of structural responses by capturing a broader spectrum of structural responses for comprehensive design considerations. Although this method is less intuitive, it is a reliable method and computationally efficient [25-27].

It is worth mentioning that almost all of the above-mentioned studies and most of the well-known published evidence in the literature of ***SHM*** by wavelet transformation analysis are reported for steel structures [2, 4, 18, 24, 26-30]. The evaluation of damage diagnosis by ***WB-DSF*** for reinforced concrete buildings has not been comprehensively investigated. It was shown by many researchers that the continuous wavelet transform (***CWT***) functions are efficient in revealing inconsistencies in structural responses. The continuous wavelet transform's (***CWT***) ability to provide time-frequency localization, adaptability to signal variability, multiresolution analysis, and enhanced feature extraction makes it a powerful tool for capturing non-stationary characteristics in earthquake events and structural responses, thereby justifying its widespread use in the field of structural health monitoring. Hence, this paper aims to study the effectiveness of the ***WB-DSF*** for a 4-story ***RC-MRF*** by application of an optimum ***CWT*** function (mother wavelet family). According to the author's previous studies, it has been proven that the ***bior3.3*** mother wavelet is the best among the mother wavelets investigated in this study in reinforced concrete structures. For this purpose, 2D numerical simulations of the structural models were developed in Opensees software. To diagnosis structural damage in different stories of the RC-MRF using the wavelet-based damage-sensitive feature (***WB-DSF***), floor acceleration responses were recorded for all four floors of the structure subjected to 12 ground motion records. For this purpose, nonlinear incremental dynamic analysis (***IDA***), which involved applying various scaled ground motions to assess the structure's seismic performance under different loading intensities, was used. Acceleration responses were individually analyzed for each floor, capturing the dynamic behavior and response characteristics of the structure at varying levels. This calculation procedure facilitated a comprehensive assessment of the structural performance and potential damage across all floors of the RC-MRF.

List of Abbreviations and Notations

a = Scale parameter of wavelet transform function
b = Time-shift parameter of wavelet transform function
Bior3.3 = Mother wavelet family of Biorthogonal 3.3
C1L= Low-rise concrete moment-resisting frame
CWT = Continuous wavelet transform
DS = Damage state
DS0 = Intact state
DS1 = Slight damage state
DS2 = Moderate damage state
DS3 = Extensive damage state
DS4 = Complete damage state
$E_{scale(a)}$ =Wavelet energy at a particular scale ***a***
$E_{scale(2a)}$ = Wavelet energy at particular scale ***2a***
E_{tot} = Total wavelet energy of the signal
f_1 = First natural frequency (Hz)
Fc = Central mother wavelet frequency (Hz)
$f_i(t)$ = Time-history absolute acceleration response
fn = natural frequency of structure (Hz)
fs = Sampling frequencies of the intact structure (Hz)
IDA= Incremental dynamic analysis
mean (fi(t)) = Mean value of $f_i(t)$
N = Number of data points in $f_i(t)$

RC-MRF = Reinforced concrete moment-resisting frame
RMS(fi(t)) = Root mean square of $f_i(t)$
Sa= Spectral acceleration of the first period (g)
SDR = story drift ratio
SHM =Structural Health Monitoring
T= Period (sec)
t = Time (sec)
WB-DSF = Wavelet-based damage-sensitive feature
Wf(a,b) = Continuous wavelet coefficient
Δt = Sampling time (sec)
ψ = Mother wavelet family

2. Wavelet Transformation

In this study, a normalization procedure as Equation (1) was utilized before applying the wavelet transformation to the input signal in order to use time-history acceleration responses [4, 31]. This procedure involves the subtraction of the mean value ***mean(fᵢ(t))*** from the absolute acceleration response of ***fᵢ(t)*** and dividing the resulting value (numerator) by the root mean square ***RMS(fᵢ(t))*** value (denominator). Where ***N*** is the number of data points in ***fᵢ(t)***. This procedure helps to account for different initial conditions during data collection and reduces the impact of varying loading intensities.

$$f_i(t)_{norm} = \frac{f_i(t) - mean(f_i(t))}{RMS(f_i(t))}, \qquad i = 1, ..., N \tag{1}$$

After that, the wavelet transformations of the signals were computed. The use of the ***CWT*** allows for the representation of time-varying features in the input acceleration responses of ***f(t)***, as wavelets are waves that are localized with a finite time duration. Indeed, the ***CWT*** provides the time sum of the entire ***f(t)*** signal which has been multiplied by a form of the scaled and transferred mother wavelet. This process produces a wavelet coefficient that is a function of scale and time [20]. The continuous wavelet coefficient is mathematically defined [12] as:

$$Wf(a,b) = \int_{-\infty}^{\infty} f(t) \frac{1}{\sqrt{a}} \psi^* \left(\frac{t-b}{a} \right) dt \tag{2}$$

where ***ψ*** is denoted as the mother wavelet and ***** represents a complex conjugate used to compute the wavelet coefficients of *Wf*(a,b) [12]. In Equation (2), ***f(t)*** is the time-history acceleration response, and the wavelet scale and wavelet shift in the classical application of the ***CWT*** are denoted with ***a***, and ***b***, respectively [11].

3. Wavelet Energies and Definition of Damage-Sensitive Feature

Nair and Kiremidjian [4] first introduced the concept of wavelet energy at a specific scale (***Escale(a)***). The wavelet energy correlates with the vibration energy of the acceleration response and different scales. Once, the wavelet coefficients are determined, the wavelet coefficient energy at scale ***a*** can be computed for each output signal. The energy of the wavelet coefficients is given in the following form of Equation (3) [4]:

$$E_{scale(a)} = \sum_{b=1}^{N} \left| Wf(a,b) \right|^2 \tag{3}$$

where |□| represents the absolute value of the quantity, and other parameters were previously defined. It can be seen that the ***Escale(a)*** is the sum of all wavelet coefficients over the time history of accelerations at scale ***a***. In a discrete time-series acceleration response, the relation for scale ***a*** can be expressed as follows [2]:

$$a = f_s \frac{F_c}{f_n}, \qquad f_s = \frac{1}{\Delta t} \tag{4}$$

where F_c, f_s, and f_n, are the central mother wavelet frequency, sampling, and natural frequencies of the intact structure, and ***Δt*** is the sampling time, respectively. By using the mathematical relations of energy of wavelet coefficients, ***WB-DSF*** can be extracted from wavelet energies to predict the damage states in structures. The ***WB-DSF*** illustrates the relationship between the wavelet energy at the natural frequency and the progress of damage incidence in the structure. Equation (5) represents the mathematical expression of the ***WB-DSF.***

$$WB - DSF = \frac{E_{scale(a)}}{E_{tot}} \tag{5}$$

where E_{tot} is the sum of the wavelet energies at scales ***a*** and ***2a*** that correspond to the first and half of the first natural frequency of the intact structure, and $E_{scale(a)}$ is defined, previously. Hence, the total energy has the following form of Equation (6):

$$E_{tot} = E_{scale(a)} + E_{scale(2a)} \tag{6}$$

In the normalized form of ***WB-DSF***, this value varies between 0 and 1, i.e., ***0≤WB-DSF≤1***.
It is worth mentioning that the conventional form of ***WB-DSF*** was utilized in this study. The conventional wavelet-based damage-sensitive feature yields more accurate assessments of the damage state (DS) in low-rise buildings, while the counterpart refined form of the wavelet-based damage-sensitive feature is more appropriate for capturing higher-mode contributions in mid-rise and high-rise buildings. Given that the focus is on diagnosing structural damage in a 4-story reinforced concrete moment-resisting frame with special ductility, classified as a low-rise building according to HAZUS MR5 instructions, the conventional ***WB-DSF*** was employed. The decision to utilize the conventional wavelet-based DSF for the low-rise reinforced concrete moment resisting frame was driven by its proven capability to capture primary damage indicators associated with low-frequency responses, aligning with the structural

characteristics, seismic behavior, and design considerations of the building under investigation. This choice was made to ensure precise and efficient damage diagnosis tailored to the specific requirements of low-rise structures with special ductility designs.

To enhance comprehension and streamline the calculation procedures in this study, a flowchart was depicted (Figure 1) that outlines the problem definition, analysis methods, software used, and output. In summary, the calculation procedure of this study comprises the following steps.

1. Nonlinear Incremental Dynamic Analysis (***IDA***): The study initiated with Nonlinear Incremental Dynamic Analysis (***IDA***) to assess the structural response of the ***RC-MRF*** subjected to ground motion stimulation.

2. Application of Wavelet Transformation to Acceleration Responses: Following the ***IDA***, wavelet transformation was applied to the recorded floor acceleration responses of all four floors of the ***RC-MRF***. By applying wavelet transformation to the acceleration responses, the study aimed to extract relevant features and patterns associated with structural dynamics and damage diagnosis.

3. Calculation of Energy of Wavelet Coefficients: After obtaining the wavelet coefficients through transformation, the energies of these coefficients were calculated. By quantifying the energy content of wavelet coefficients, the study sought to identify key features and variations indicative of structural damage.

4. Derivation of wavelet-based Damage-Sensitive Feature (***WB-DSF***) from Wavelet Coefficients: Based on the wavelet coefficients of acceleration signals and their energy characteristics, damage-sensitive features (***WB-DSF***) were derived. ***WB-DSF*** is a specific indicator that captures changes in signal properties associated with structural damage. By analyzing the wavelet coefficients and extracting DSF, the research aimed to develop effective tools for classifying or predicting structural damage in ***RC-MRF*** using wavelet-based techniques.

4. Numerical Simulation of a 4-Story Special RC-MRF

To evaluate the robustness and efficiency of the ***WB-DSF*** for damage diagnosis, the 2D model of a 4-story reinforced concrete moment-resisting frame with special ductility was utilized. Detailed descriptions of the under-hand numerical model can be found in the seminal studies of Haselton and Deierlein [32]. Table 1 and Figure 2 demonstrate the configuration and dimensions of the under-consideration frame of the current study. The building frame was designed by IBC-2003 [33], ASCE7-02 [34], and ACI 318-02 [35].

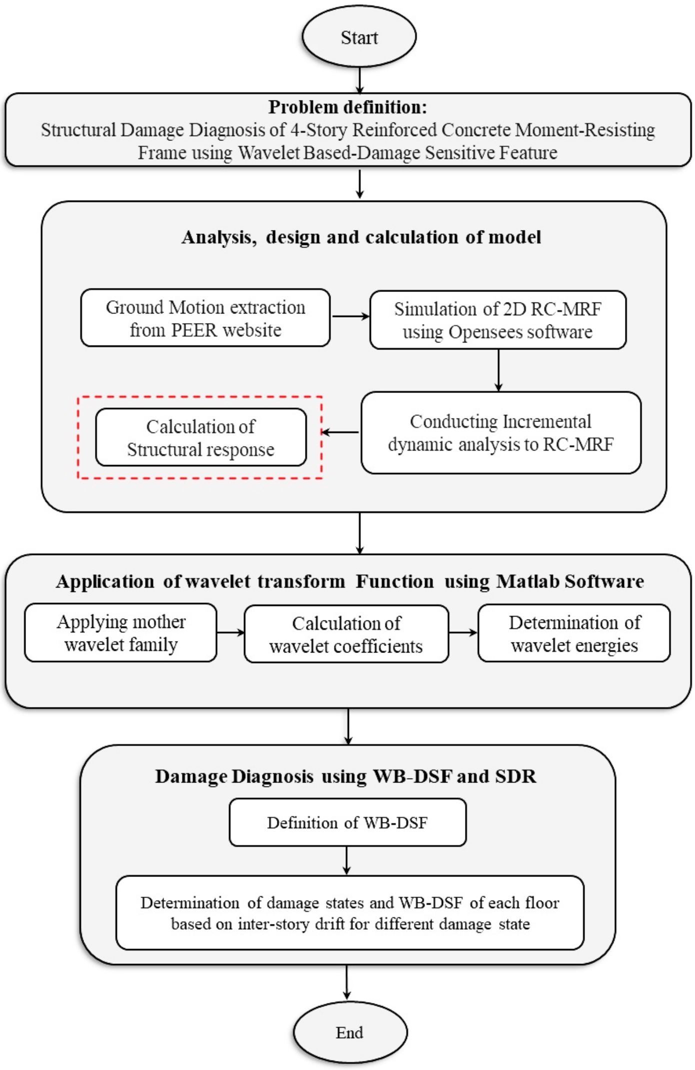

Fig. 1: Flowchart of calculation procedure.

Table 1: Representative building geometries and dimensions [32].

Number of stories	First story height ft(m)	Upper story height ft (m)	Number of spans	Spans' length ft (m)
4	15 (4.57)	13 (3.96)	3	20 (6.09)

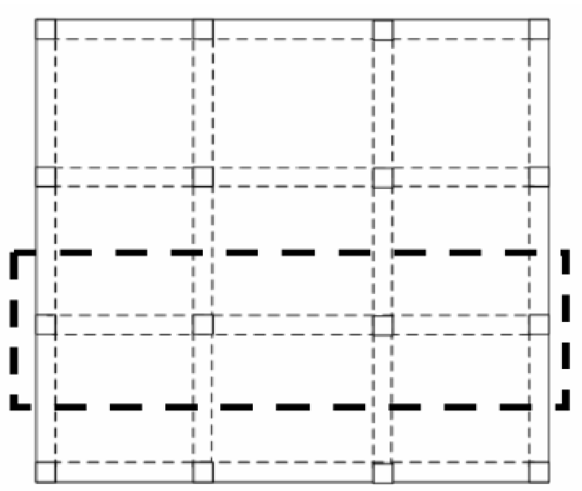

Fig. 2: Plan of the 4-story RC-MRF.

The 2D model of the frame was constructed in Opensees software [36], and absolute acceleration responses were extracted at the floors of ***RC-MRF*** using incremental dynamic analysis (***IDA***) [15, 16]. The concentrated plasticity approach which was comprehensively presented in the study of Ibarra [37], Medina and Krawinkler [38], Haselton and Deierlein [32], and Moehle et al. [39] was applied to model the inelastic behavior of the beams. To numerically simulate the above-mentioned concentrated plasticity approach, it was hypothesized that a beam-column element with linear elasticity would be used for each beam, and two rotational springs of negligible length would be employed to represent plastic hinges at either end of the beam. It is worthwhile noting that the modeled frame has a peripheral lateral resisting system. The modified Ibarra-Krawinkler model, as described by Lignos and Krawinkler [40], was utilized in the model to account for component deterioration. The building frames were subjected to 12 ground motion records whose characteristics are reported in Table 2.

5. Results and Discussion

5.1 Nonlinear incremental dynamic analysis (IDA)

By simulating the 4-story ***RC-MRF*** in Opensees software [36], an incremental dynamic analysis (IDA) was conducted and the absolute acceleration responses of floors were extracted. To verify the calculation procedure, the first mode period times of 4-story reinforced concrete frames were compared with those of Haselton and Deierlein [32]. It can be concluded from Table 3 that the period times of the 4-Story ***RC-MRF*** are in good consistency with each other.

The story drift ratios of the building frame were calculated till the structural failures occurred. To ensure the structure collapses under the seismic ground motions, a threshold value for maximum story drift ratio (***SDR***) was assumed. In other words, the calculation of acceleration responses in ***IDA*** involves applying ground motion records, simulating dynamic responses, and monitoring structural behavior until reaching the predefined drift limit, enabling engineers to assess structural performance and enhance seismic design practices. This threshold value of the maximum story drift ratio in ***IDA*** is a crucial parameter that influences the analysis outcomes and provides insights into the structural response under seismic loading. Pakzad and Fenves [41] and Hwang [42] proposed a value of ***SDR=0.1*** for the maximum story drift ratio. During the ***IDA*** process, the acceleration responses of the structure were computed until the maximum story drift ratio reached its threshold value. After that, the Hunt and Fill algorithm was utilized to find the collapse point of each structure [43]. Figure 3 demonstrates the ***IDA*** curves of the 4-story ***RC-MRF***.

Table 2: The characteristics of ground motion records.

Event Information							Site Information				Record Info.
EQ No.	**EQ ID**	**PEER Rec. Num.**	**Mag.**	**Year**	**Event**	**Fault Type**	**Station Name**	**Vs_30 (m/s)**	**Campbell Distance (km)**	**Joyner- Boore Distance (km)**	**Lowest Useable Freq. (Hz)**
1	12011	953	6.7	1994	Northridge	Blind thrust	Beverly Hills - 14145 Mulhol	356	17.2	9.4	0.25
2	12012	960	6.7	1994	Northridge	Blind thrust	Canyon Country - W Lost Cany	309	12.	11.4	0.13
3	12013	1003	6.7	1994	Northridge	Blind thrust	LA - Saturn St	309	27.0	21.2	0.13
4	12015	952	6.7	1994	Northridge	Blind thrust	Beverly Hills - 12520 Mulhol	546	18.4	12.4	0.16
5	12041	1602	7.1	1999	Duzce, Turkey	Strike-slip	Bolu	326	12.4	12.0	0.06
6	12052	1787	7.1	1999	Hector Mine	Strike-slip	Hector	685	12.0	10.4	0.04
7	12061	169	6.5	1979	Imperial Valley	Strike-slip	Delta	275	22.5	22.0	0.06
8	12062	174	6.5	1979	Imperial Valley	Strike-slip	El Centro Array #11	196	13.5	12.5	0.25
9	12063	162	6.5	1979	Imperial Valley	Strike-slip	Calexico Fire Station	231	11.6	10.5	0.25
10	12071	1111	6.9	1995	Kobe, Japan	Strike-slip	Nishi-Akashi	609	25.2	7.1	0.13
11	12072	1116	6.9	1995	Kobe, Japan	Strike-slip	Shin-Osaka	256	28.5	19.1	0.13
12	12073	1107	6.9	1995	Kobe, Japan	Strike-slip	Kakogawa	312	3.2	22.5	0.13

Table 3: Comparison of period time of the RC-MRF.

No. of stories	First Mode Period (T_1) [sec]	
	Haselton and Deierlein [32]	Current study
4	0.94	0.93

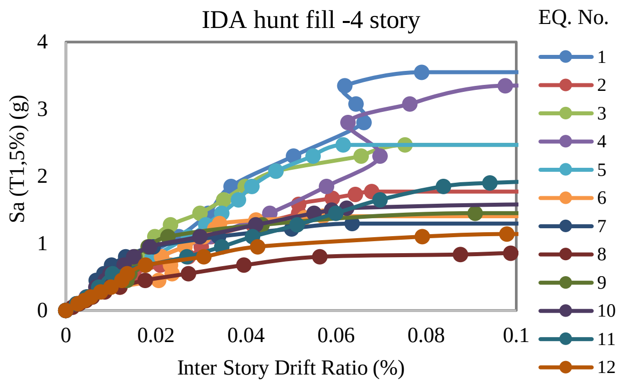

Fig. 3: IDA curves of the 4-story building frame.

To classify the damage states (***DS***) of structures, the absolute acceleration measurements were correlated with story drift values (***SDR***). The estimation of the extent of damage was calculated based on the maximum induced ***SDR*** of the frames. Consequently, some threshold values for ***SDR*** are assumed for different defined damage states (***DSi***) reported in the HAZUS MR5 instructions. These values are given in Table 4 [44].

Table 4: Determination of damage state based on story drift values [44].

Building Type			Threshold inter-story drift for different damage state			
C1L	Height (inches)		DS1	DS2	DS3	DS4
	Roof	Modal	Slight	Moderate	Extensive	Complete
	600	450	0.0033	0.0058	0.0156	0.04

5.2 Applying wavelet transformation to the outputs of acceleration responses

To detect structural damages of the 4-story ***RC-MRF***, wavelet transformation was used. For this purpose, the first natural frequency of the intended frame, f_1 at the intact state (***DS0***) should be found. The time-based calculation of wavelet energy at scale a corresponds to frequency (f_1). Figure 4.a demonstrates the wavelet transformation analysis at ***DS0*** in the form of 3D distribution curves of wavelet coefficients versus scale-time and energy of the wavelet coefficient of the 4-story building subjected to the Kobe Japan 1995, Nishi-Akashi station excitation. The maximum wavelet energies and corresponding scales in the case of an intact state (***DS0***) can be also seen in Figure 3.b. It is worthwhile to mention that 2D and 3D representations of wavelet coefficients/energy versus time and scale of the 4-story building frame subjected to the Kobe Japan 1995, Nishi-Akashi station excitation were provided as an unlimited example, and for conciseness, the findings of other seismic ground motions were reported in the following sections.

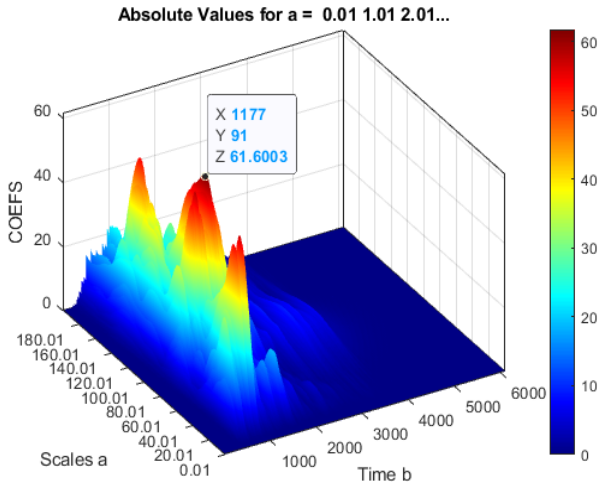

(a)

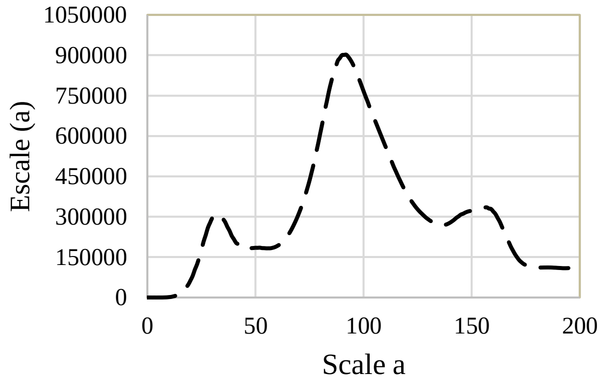

(b)

Fig. 4: Wavelet transformation analysis at DS0 for 4-story building; a) 3D distribution curves of wavelet coefficients versus scale-time, b) Energy of the wavelet coefficient under Kobe Japan 1995, Nishi-Akashi.

The predominant period of the structure at the intact state of ***DS0*** can be found by using the time history of the absolute acceleration response and the application of Seismosignal software. Then, the scale value attributed to the energy of the wavelet coefficients can be extracted. Figure 5 illustrates the predominant period of the 4-story frame under the Kobe Japan 1995, Nishi-Akashi earthquake. By calculating the predominant period of the structure at the intact state and corresponding scale, the energy of the wavelet coefficients and other parameters dependent on the energy of the coefficients, including the ***WB-DSF*** can be found. Table 5 shows the predominant period of the structure in the intact state and the scale of the 4-story building subjected to the Kobe Japan 1995, Nishi-Akashi station excitation.

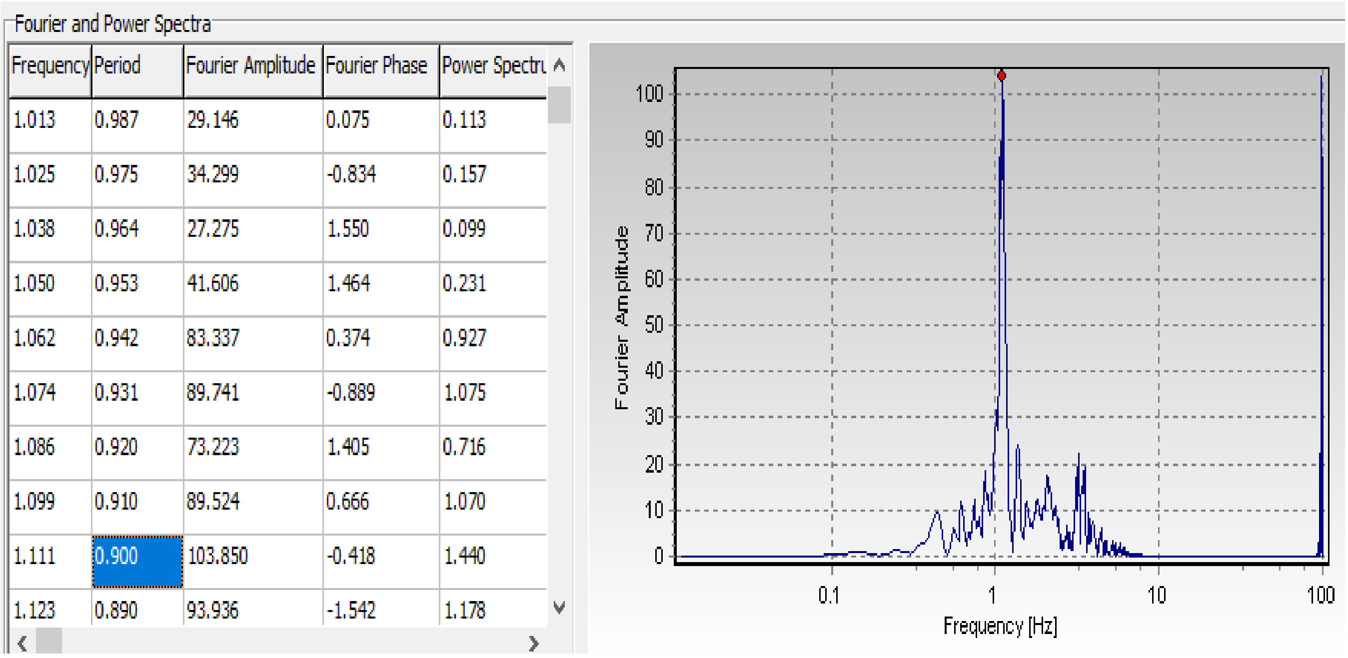

Fig. 5: Predominant period at DS0 of the 4-story building under Kobe Japan 1995, Nishi-Akashi.

Table 5: Predominant period time and the scale ***a*** at the intact state of the building.

Name of record	No. of stories	T (Seismosignal) [sec]	Scale *a* (Seismosignal)	Scale *a* (Max wavelet diagram)
Kobe Japan 1995, Nishi-Akashi	4	0.9	90	91.00

5.3 Derivation WB-DSF Using Wavelet Coefficients of Acceleration Signals

Superimposed in Figure 6 is the variation of ***WB-DSF*** values based on the time-histories response of absolute acceleration for different damage states (***DS****i*) at each floor of the 4-story building frame under the Kobe Japan 1995, Nishi-Akashi ground motion. It can be seen from Figure 6 that if the building frame is intact (i.e., ***DS0***), the ***WB-DSF*** value is higher than ***0.9***. As the damage progresses in the building frame, the ***WB-DSF*** values gradually decrease, which indicates how the energy alters to a higher scale. With increasing the level of damage state, the wavelet energy diminishes at a scale matching the initial natural frequency of the intact structure. Therefore, damage that occurs in the severe intensities of the input ground motion is more probable at the ***DS4***. This is due to the fact that according to the HAZUS MR5 instructions, ***DS4*** is related to complete damage. Another observation is that the variation rate of ***WB-DSF*** during ***DS2*** to ***DS3*** is impressive in comparison to the previous damage states range (sudden changes in ***WB-DSF***). Therefore, it can be concluded that the nonlinear damages progressively initiate in the building frame at the end of ***DS2***. As the intensity of the earthquake increases, ***WB-DSF*** has the lowest values on the first floor, so the occurrence of damage on the first floor is more likely in extreme intensities. This observation can be related to the occurrence of the maximum ***SDR*** as shown in Table 6 on the first floor.

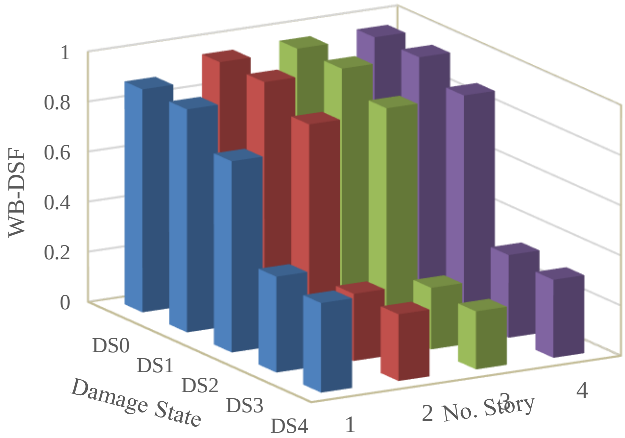

Fig. 6: Variation of WB-DSF for 4-story building frame under Kobe Japan 1995, Nishi-Akashi.

Table 6: Variation of SDR of the 4-story building frame under Kobe Japan 1995, Nishi-Akashi.

Damage state	Drift			
	Story 1	Story 2	Story 3	Story 4
DS0	0.0013	0.0011	0.0008	0.0005
DS1	0.0026	0.0022	0.0017	0.0010
DS2	0.0063	0.0066	0.0057	0.0030
DS3	0.0198	0.0267	0.0297	0.0226
DS4	0.0551	0.0475	0.0469	0.0348

Table 7 illustrates the values of ***WB-DSF*** and story drift ratio of the 4-story building frame under 12 ground motion records with different values of spectral acceleration response (***Sa***). The results show that ***WB-DSF*** has the lowest values on the first floor, so the occurrence of damage on the first floor is more likely in severe intensities. The values of ***WB-DSF*** of the 4-story building frame under 12 ground motion records were reported in Table 7. It can be observed from Table 7 that the maximum ***SDR*** occurs on the first floor of a 4-story building for all of the earthquake ground motions. So, it can be deduced that a higher value of the maximum drift ratio yields a lower value of ***WB-DSF***.

Table 7: Variation of WB-DSF at different intensities of the 4-story building frame under 12 ground motion records.

Record	Sa	story 1		story 2		story 3		story 4	
		drift	WB-DSF	drift	WB-DSF	drift	WB-DSF	drift	WB-DSF
Northridge 1994, Beverly Hills	0.1	0.00266	0.9788	0.002376	0.9902	0.001771	0.9918	0.000939	0.9918
	0.2	0.0052	0.9717	0.004489	0.9877	0.003033	0.99	0.001586	0.9902
	0.35	0.00753	0.9258	0.006752	0.9667	0.004034	0.974	0.001921	0.9755
	0.8	0.01718	0.6195	0.013761	0.7942	0.007518	0.8437	0.002735	0.8523
	1.1	0.02507	0.5185	0.020773	0.7008	0.011029	0.7741	0.003181	0.7887
	2.3	0.04455	0.5617	0.05054	0.4616	0.039471	0.5782	0.00535	0.6136
Northridge 1994, Canyon Country	0.1	0.00244	0.7396	0.002193	0.8474	0.001548	0.8485	0.000814	0.8446
	0.2	0.00487	0.7087	0.004532	0.8201	0.003018	0.8206	0.001598	0.818
	0.35	0.00827	0.5989	0.008227	0.6983	0.004713	0.6861	0.002358	0.6963
	0.675	0.01943	0.265	0.020955	0.2486	0.015305	0.2028	0.003698	0.2583
	0.8	0.02718	0.16	0.026032	0.1443	0.020124	0.1346	0.00485	0.1707
	1.58	0.05014	0.191	0.00485	0.1956	0.043805	0.2081	0.015717	0.2364
	1.67	0.05727	0.1947	0.059123	0.1945	0.048201	0.2074	0.016541	0.2395
Northridge 1994, LA - Saturn	0.1	0.00256	0.9215	0.002186	0.9677	0.001666	0.9663	0.000958	0.9602
	0.2	0.00481	0.8988	0.000958	0.9579	0.003296	0.9565	0.001867	0.949
	0.35	0.00679	0.8108	0.007812	0.9142	0.005747	0.9145	0.002896	0.9053
	0.55	0.00883	0.7045	0.010354	0.8579	0.008712	0.8778	0.003774	0.8719
	1.275	0.01747	0.3968	0.022309	0.4655	0.02221	0.5194	0.005437	0.5298
	1.45	0.02974	0.4056	0.025912	0.4333	0.025419	0.4827	0.005239	0.494
	2.075	0.04661	0.4399	0.037922	0.4473	0.037293	0.5073	0.006803	0.5134
	2.3	0.06556	0.437	0.053462	0.4457	0.042063	0.4954	0.00743	0.5075
Northridge 1994, Beverly Hills	0.1	0.00233	0.8274	0.002122	0.9546	0.001681	0.9755	0.001053	0.9558
	0.2	0.00452	0.7844	0.004355	0.9359	0.003154	0.9638	0.002081	0.9376
	0.35	0.00646	0.6282	0.007984	0.8294	0.005792	0.897	0.003482	0.8467
	0.8	0.01943	0.3715	0.020512	0.3621	0.020831	0.5876	0.013611	0.5039
	1.45	0.04383	0.4625	0.045305	0.3417	0.040597	0.4418	0.028907	0.4466
	1.85	0.05262	0.5233	0.057875	0.3713	0.051521	0.3911	0.033454	0.4334
	2.3	0.05885	0.5233	0.069545	0.3795	0.069759	0.445	0.039617	0.4938
Duzce Turkey 1999	0.1	0.00292	0.9457	0.002337	0.9759	0.001673	0.9796	0.001089	0.9792
	0.2	0.00581	0.9206	0.004269	0.9622	0.003292	0.9682	0.002063	0.9686
	0.35	0.00955	0.8432	0.007411	0.9018	0.005436	0.91	0.002717	0.9181
	0.8	0.01915	0.6043	0.015019	0.62	0.007038	0.5549	0.004025	0.6436
	1.1	0.02721	0.4279	0.023249	0.4368	0.010089	0.3758	0.003914	0.4626
	2.075	0.04664	0.2574	0.045386	0.2567	0.023403	0.2626	0.009202	0.3026
	2.3	0.05485	0.2476	0.052805	0.2589	0.026506	0.2668	0.00768	0.3005

continued on next page

Table 7 (continued)

Record	Sa	story 1		story 2		story 3		story 4	
		drift	WB-DSF	drift	WB-DSF	drift	WB-DSF	drift	WB-DSF
Hector Mine 1999	0.1	0.00276	0.9035	0.002426	0.9576	0.001787	0.9679	0.000989	0.9681
	0.2	0.00493	0.8866	0.0044668	0.9483	0.003147	0.9603	0.001781	0.9608
	0.35	0.01199	0.7183	0.010045	0.807	0.005402	0.8334	0.002382	0.8364
	0.45	0.02062	0.5343	0.016368	0.6025	0.007424	0.6372	0.00282	0.6572
	0.675	0.02325	0.3789	0.021487	0.401	0.012292	0.4412	0.003294	0.4549
	1.1	0.03065	0.4312	0.029656	0.3985	0.015799	0.4563	0.004176	0.4759
	1.34	0.04222	0.4368	0.032767	0.3412	0.017819	0.3996	0.004343	0.4228
	1.38	0.05293	0.4375	0.032771	0.3339	0.017807	0.3919	0.004329	0.4159
Imperial Valley 1979, Delta	0.1	0.00284	0.8902	0.002844	0.9514	0.001973	0.9631	0.001153	0.9647
	0.15	0.00424	0.8749	0.003599	0.9444	0.002539	0.9577	0.00146	0.9595
	0.275	0.00676	0.815	0.006086	0.9112	0.003925	0.9315	0.002013	0.9353
	0.35	0.00706	0.7656	0.006594	0.8819	0.004394	0.9084	0.002218	0.9145
	0.675	0.01015	0.5575	0.009196	0.6691	0.006482	0.7153	0.003114	0.7497
	0.95	0.01941	0.4284	0.013302	0.5056	0.008122	0.5488	0.003688	0.5995
	1.21	0.05012	0.332	0.027946	0.4105	0.012756	0.4719	0.004776	0.5135
	1.29	0.06356	0.2643	0.060708	0.2976	0.012267	0.344	0.005644	0.3881
Imperial Valley 1979, El Centro Array #11	0.1	0.00295	0.7843	0.002269	0.869	0.002301	0.8889	0.001552	0.9015
	0.15	0.00443	0.7524	0.004425	0.8365	0.003219	0.8544	0.00216	0.8737
	0.2	0.0059	0.7019	0.004531	0.7828	0.003867	0.7931	0.002682	0.825
	0.275	0.00861	0.5962	0.006859	0.6405	0.005077	0.6059	0.003353	0.6797
	0.45	0.01762	0.3997	0.014528	0.3889	0.007661	0.3167	0.003918	0.3981
	0.55	0.02724	0.3218	0.022847	0.3429	0.010484	0.261	0.004414	0.3481
	0.8	0.05635	0.269	0.052016	0.3026	0.018024	0.2614	0.005926	0.3385
Imperial Valley 1979, Calexico Fire Station	0.1	0.00242	0.8817	0.002226	0.9315	0.001795	0.9363	0.00125	0.9266
	0.2	0.00474	0.8809	0.004466	0.9313	0.003307	0.936	0.002305	0.9263
	0.275	0.00741	0.8655	0.005999	0.921	0.00402	0.9252	0.002588	0.9161
	0.45	0.01359	0.7179	0.011332	0.7888	0.007242	0.7882	0.004007	0.791
	0.95	0.01822	0.4582	0.017162	0.4262	0.015357	0.4464	0.013003	0.4654
	1.1	0.02268	0.4578	0.022236	0.3835	0.021005	0.4137	0.018115	0.4279
	1.275	0.04358	0.4477	0.037863	0.401	0.027005	0.4171	0.018453	0.4454
Kobe Japan 1995, Nishi-Akashi	0.1	0.0026	0.8901	0.002291	0.9527	0.001748	0.9605	0.001042	0.9599
	0.2	0.00464	0.8539	0.004262	0.931	0.003139	0.9412	0.001961	0.9414
	0.275	0.00634	0.7628	0.006674	0.8639	0.005709	0.8821	0.003007	0.8871
	0.45	0.00778	0.6938	0.008742	0.7883	0.007381	0.8072	0.003458	0.8228
	0.95	0.01495	0.3633	0.018588	0.3269	0.016949	0.3592	0.010916	0.4338
	1.1	0.0198	0.3823	0.026721	0.2674	0.029756	0.2452	0.022619	0.33
	1.275	0.05512	0.3572	0.047578	0.266	0.04694	0.2534	0.03484	0.3113
	1.45	0.06237	0.3541	0.0514	0.2598	0.045806	0.2497	0.031927	0.3036
Kobe Japan 1995, Shin-Osaka	0.1	0.00238	0.8683	0.002144	0.9325	0.001577	0.9309	0.00088	0.9256
	0.2	0.00465	0.8469	0.004309	0.9187	0.003013	0.9168	0.001628	0.9108
	0.35	0.00728	0.7967	0.007067	0.8845	0.004579	0.8841	0.002362	0.8777
	0.55	0.01007	0.6613	0.01032	0.767	0.005799	0.7785	0.002603	0.7792
	0.8	0.02687	0.4783	0.025321	0.5519	0.014003	0.5971	0.003267	0.6109
	0.95	0.03459	0.4483	0.03311	0.4799	0.021309	0.5268	0.004049	0.554
	1.1	0.04146	0.4306	0.040456	0.4379	0.027062	0.4908	0.004874	0.5264
	1.275	0.05132	0.4147	0.050431	0.4073	0.029995	0.4676	0.005329	0.5106
	1.45	0.05994	0.4032	0.059728	0.3704	0.0352	0.4403	0.00588	0.4843

continued on next page

Table 7 (continued)

Record	Sa	story 1		story 2		story 3		story 4	
		drift	WB-DSF	drift	WB-DSF	drift	WB-DSF	drift	WB-DSF
Kobe Japan 1995, Kakogawa	0.1	0.00268	0.8421	0.002144	0.8967	0.00152	0.9139	0.000914	0.9182
	0.2	0.00551	0.8407	0.004371	0.8953	0.00293	0.9127	0.001782	0.9172
	0.275	0.00773	0.8479	0.006386	0.9035	0.003827	0.9205	0.002346	0.925
	0.35	0.01	0.8078	0.008341	0.8709	0.005538	0.8925	0.00305	0.9011
	0.45	0.0124	0.7101	0.009729	0.7787	0.005786	0.8101	0.003379	0.8276
	0.55	0.01365	0.6135	0.011951	0.657	0.007264	0.6904	0.003638	0.7202
	0.675	0.01769	0.5248	0.01626	0.4982	0.009634	0.5057	0.00381	0.5564
	0.8	0.0306	0.4438	0.023821	0.3593	0.009556	0.333	0.00436	0.3971
	0.95	0.04259	0.4618	0.029518	0.4204	0.011732	0.4423	0.003719	0.4865

6. Summary and Conclusions:

In this study, the ***WB-DSF*** for ***RC-MRFs*** was extracted based on wavelet energies. Furthermore, the theoretical correlation between the output of wavelet analysis and dynamic structural behaviors that play a vital role in damage detection methods was derived. For this purpose, absolute acceleration responses recorded at each story level of the 4-story concrete MRF were extracted using incremental dynamic analysis (***IDA***) by use of 12 seismic ground motion records to formulate the damage states. Then, ***WB-DSF*** was extracted from the absolute acceleration responses of ***RC-MRFs*** by using the ***Bior3.3*** mother wavelet transform functions. From the findings of this study, the following results can be pointed out:

- As the damage progresses in the 4-story building frame, the ***WB-DSF*** values gradually decrease, which indicates how the wavelet energy moves to a higher scale.
- As the level of damage states increases, the wavelet energy decreases at a scale that corresponds to the first natural frequency of the intact frame. This finding is significant in developing effective damage detection techniques. Furthermore, the damage that occurs in the severe intensities of the input ground motion is more probable at the ***DS4***. This is due to the fact that according to the HAZUS MR5 instructions, ***DS4*** is related to complete damage.

The impressive variation rate and sudden changes of ***WB-DSF*** from ***DS2*** to ***DS3*** can be related to the initiation of progressive nonlinear damages at the end of ***DS2***.

Disclosure Statement

No potential conflict of interest was reported by the authors.

References

[1] Noh, H. Y., Nair, K. K., Lignos, D. G. & Kiremidjian, A. S. 2011. Use of wavelet-based damage-sensitive features for structural damage diagnosis using strong motion data. *Journal of Structural Engineering,* 137, 1215-1228.

[2] Yazdanpanah, O., Mohebi, B. & Yakhchalian, M. 2020. Selection of optimal wavelet-based damage-sensitive feature for seismic damage diagnosis. *Measurement,* 154, 107447.

[3] Mahin, S. A. 1998. Lessons from damage to steel buildings during the Northridge earthquake. *Engineering structures,* 20, 261-270.

[4] Nair, K. & Kiremidjian, A. 2007. Damage diagnosis algorithm for wireless structural health monitoring. *Rep. No. 165*. John A. Blume Earthquake Engineering Center: Department of Civil Engineering, Stanford University.

[5] Bayissa, W., Haritos, N. & Thelandersson, S. 2008. Vibration-based structural damage identification using wavelet transform. *Mechanical systems and signal processing,* 22, 1194-1215.

[6] Panahi Boroujeni, M., Zareei, S.A., Birzhandi, M.S. & Zafarani, M.M. 2024. Development of Seismic Fragility Functions for Reinforced Concrete Buildings Using Damage-Sensitive Features Based on Wavelet Theory. *Structural Control and Health Monitoring*, 2024(1), 8754191-8754212.

[7] Fan, W. & Qiao, P. 2011. Vibration-based damage identification methods: a review and comparative study. *Structural health monitoring,* 10, 83-111.

[8] Hera, A. & Hou, Z. 2004. Application of wavelet approach for ASCE structural health monitoring benchmark studies. *Journal of Engineering Mechanics,* 130, 96-104.

[9] Nair, K. K. & Kiremidjian, A. S. 2009. Derivation of a damage sensitive feature using the Haar wavelet transform. *Journal of Applied Mechanics,* 76, 061015-061024.

[10] Aguirre, D. A., Gaviria, C. A. & Montejo, L. A. 2013. Wavelet-based damage detection in reinforced concrete structures subjected to seismic excitations. *Journal of Earthquake Engineering,* 17, 1103-1125.

[11] Balafas, K. & Kiremidjian, A. S. 2015. Development and validation of a novel earthquake damage estimation scheme based on the continuous wavelet transform of input and output acceleration measurements. *Earthquake Engineering & Structural Dynamics,* 44, 501-522.

[12] Mallat, S. 1999. *A wavelet tour of signal processing*, Elsevier.

[13] Cruz, P. J. & Salgado, R. 2009. Performance of vibration-based damage detection methods in bridges. *Computer-Aided Civil and Infrastructure Engineering,* 24, 62-79.

[14] Solís, M., Algaba, M. & Galvín, P. 2013. Continuous wavelet analysis of mode shapes differences for damage detection. *Mechanical Systems and Signal Processing,* 40, 645-666.

[15] Vamvatsikos, D. & Cornell, C. A. 2002. Incremental dynamic analysis. *Earthquake engineering & structural dynamics,* 31, 491-514.

[16] Vamvatsikos, D. 2002. *Seismic performance, capacity and reliability of structures as seen through incremental dynamic analysis.* Ph.D. dissertation, Stanford University.

[17] Noh, H., Nair, K., Lignos, D. & Kiremidjian, A. Application of Wavelet Coefficient Energies of Stationary and Non-Stationary Response Signals for Structural Damage Diagnosis. Proceedings of the 7th International Workshop on Structural Health Monitoring, Stanford, CA, USA, 2009. 9-11.

[18] Nair, K. K. & Kiremidjian, A. S. 2009. Derivation of a damage sensitive feature using the Haar wavelet transform.

[19] Hou, Z., Noori, M. N. & St Amand, R. 2000. Wavelet-based approach for structural damage detection. *Journal of Engineering mechanics,* 126, 677.

[20] Ghanem, R. & Romeo, F. 2000. A wavelet-based approach for the identification of linear time-varying dynamical systems. *Journal of sound and vibration,* 234, 555-576.

[21] Jamshidi Chenari, R. & Izadi., A. 2019. Discussion of "An Analytical Probabilistic Analysis of Slopes Based on Limit Equilibrium Methods" by A. Johari, S. Mousavi, November 2018. *Bulletin of Engineering Geology and the Environment*, 78, 5511–5515.

[22] Noh, H., Nair, K., Lignos, D. & Kiremidjian, A. Application of Wavelet Coefficient Energies of Stationary and Non-Stationary Response Signals for Structural Damage Diagnosis. Proceedings of the 7th International Workshop on Structural Health Monitoring, 2009 Stanford, CA, USA. 9-11.

[23] Mikami, S., Beskhyroun, S. & Oshima, T. 2011. Wavelet packet based damage detection in beam-like structures without baseline modal parameters. *Structure and Infrastructure Engineering,* 7, 211-227.

[24] Hwang, S.-H. & Lignos, D. G. 2018. Assessment of structural damage detection methods for steel structures using full-scale experimental data and nonlinear analysis. *Bulletin of Earthquake Engineering,* 16, 2971-2999.

[25] Noh, H. 2011. *Damage diagnosis algorithms using statistical pattern recognition for civil structures subjected to earthquakes,* Stanford University.

[26] Noh, H., Krishnan Nair, K., Lignos, D. G. & Kiremidjian, A. S. 2011. Use of wavelet-based damage-sensitive features for structural damage diagnosis using strong motion data. *Journal of Structural Engineering,* 137, 1215-1228.

[27] Yazdanpanah, O., Mohebi, B. & Yakhchalian, M. 2020. Seismic damage assessment using improved wavelet-based damage-sensitive features. *Journal of Building Engineering,* 31, 101311.

[28] Lignos, D. 2008. *Sidesway collapse of deteriorating structural systems under seismic excitations,* Stanford University.

[29] Noh, H. Y., Lignos, D. G., Nair, K. K. & Kiremidjian, A. S. 2012. Development of fragility functions as a damage classification/prediction method for steel moment-resisting frames using a wavelet-based damage sensitive feature. *Earthquake Engineering & Structural Dynamics,* 41, 681-696.

[30] Hwang, S.-H. & Lignos, D. G. 2018. Nonmodel-based framework for rapid seismic risk and loss assessment of instrumented steel buildings. *Engineering Structures,* 156, 417-432.

[31] Noh, H. Y. 2013. *Damage diagnosis algorithms using statistical pattern recognition for civil structures subjected to earthquakes.* Ph.D. dissertation, Stanford University.

[32] Haselton, C. B. & Deierlein, G. G. 2008. Assessing seismic collapse safety of modern reinforced concrete moment frame buildings. *PEER Report 2007/08.* Pacific Earthquake Engineering Research Center College of Engineering: University of California.

[33] ICC 2003. International Building Code 2003. International Code Council, University of Michigan, VA.

[34] ASCE 2002. Minimum Design Loads for Buildings and Other Structures; ASCE-7-02. American Society of Civil Engineers, Reston, VA.

[35] ACI 2002. Building Code Requirements for Structural Concrete (ACI 318-02) and Commentary (ACI 318R-02). American Concrete Institute, Farmington Hills, MI.

[36] McKenna, F. 2011. OpenSees: a framework for earthquake engineering simulation. *Computing in Science & Engineering,* 13, 58-66.

[37] Ibarra, L. F. 2004. *Global collapse of frame structures under seismic excitations*, Stanford University.

[38] Medina, R. A. & Krawinkler, H. 2005. Evaluation of drift demands for the seismic performance assessment of frames. *Journal of Structural Engineering,* 131, 1003-1013.

[39] Moehle, J. P., Mahin, S. & Bozorgnia, Y. 2010. Modeling and acceptance criteria for seismic design and analysis of tall buildings. *PEER Report 2010,* 111.

[40] Lignos, D. & Krawinkler, H. 2009. Sidesway collapse of deteriorating structural systems under seismic excitations. Report No. TB 172, John A. Blume Earthquake Engineering Research Center, Department of Civil and Environmental Engineering. *Department of Civil and Environmental Engineering.*

[41] Pakzad, S. N. & Fenves, G. L. 2009. Statistical analysis of vibration modes of a suspension bridge using spatially dense wireless sensor network. *Journal of Structural Engineering,* 135, 863-872.

[42] Hwang, S.-H. 2017. *Framework for earthquake-induced loss assessment of steel frame buildings-from building-specific to city-scale approaches.* Ph.D. dissertation, McGill University (Canada).

[43] Pappa, R. S., Elliott, K. B. & Schenk, A. 1993. Consistent-mode indicator for the eigensystem realization algorithm. *Journal of Guidance, Control, and Dynamics,* 16, 852-858.

[44] Agency, F. E. M. 2012. Multi-hazard loss estimation methodology HAZUS–MH 2.1 advanced engineering building module (AEBM) technical and user's manual. Federal Emergency Management Agency Washington, DC.